ISSN: 0975-8585

Research Journal of Pharmaceutical, Biological and Chemical Sciences

A Density Functional Study of the Inhibition of the Anthrax Lethal Factor Toxin by Quinoline-based small Molecules related to Aminoquinuride (NSC 12155).

Juan S. Gómez-Jeria*.

Quantum Pharmacology Unit, Department of Chemistry, Faculty of Sciences, University of Chile. Las Palmeras 3425, Santiago 7800003, Chile.

ABSTRACT

We carried out an analysis of the relationships between the electronic structure of a series of 4,6-diamino-2-methylquinoline C-6 amides related to aminoquinuride and their inhibition of the anthrax lethal factor (LF) toxin,using a model-based method. The electronic structure of all the molecules was calculated at the B3LYP/6-31g(d,p) level of theory with full geometry optimization. Linear multiple regression analysis was employed to find the best relationship between anti-LF and local atomic reactivity indices belonging to a common skeleton. The variation of the anti-LF activity is related to the variation of a set of three specific local atomic reactivity indices. A 2D partial inhibitory pharmacophore is proposed. By analyzing the process leading to a failed prediction of a molecule with a higher anti-LF activity, we show the superiority of the model-based method used here.

Keywords: Anthrax lethal factor, Local atomic reactivity indices, QSAR, pharmacophore, Quantum Chemistry, KPG method.

Corresponding author

ISSN: 0975-8585

INTRODUCTION

Anthrax is a serious infectious disease caused by *Bacillus anthracis*, a gram-positive, rod-shaped, aerobic bacterium about 1 by 9 µm in size called *Bacillus anthracis*. This was the first bacterial species shown to be the cause of a disease. Robert Koch isolated the bacteria in 1876, grew them and produced experimental anthrax by injecting them into a mouse [1-4]. Anthrax bacteria occur naturally in soil in most parts of the world and normally affect domestic and wild animals. Common hosts for anthrax comprise sheeps, cattle, horses and goats. *B. anthracis* can form latent endospores (ES) that are able to survive in harsh conditions for decades or even centuries. When ES are inhaled, ingested, or come into contact with a skin wound, they can become reactivated and the bacilli multiply quickly inside the animal or human and usually kill the host within a few days or weeks. The ES germinate at the site of entrance and the bacilli then spread by the circulation to the lymphatic system, where they reproduce. The lethality of the disease is due to the bacterium's two factors: the poly-D-glutamic acid capsule, which protects the bacterium against phagocytosis by the host neutrophils, and the protein toxin, called anthrax toxin.The bacterium-secreted toxin is composed of three protein components: a protective antigen (PA), an edema factor (EF), and a lethal factor (LF) [5]. To enter the cells, the LF and EF use the PA, which binds to two cell surface receptors on the host cell. A cell protease then cleaves the PA into two fragments: PA_{20} and PA_{63} [6]. Each PA_{63} molecule oligomerizes with six other PA_{63} fragments forming a heptameric ring-shaped arrangement [7]. In this form, the PA_{63} can competitively bind up to three EFs or LFs, forming a complex. Endocytosis takes place next and the acidified environment triggers the heptamer to liberate the LF and/or EF into the cytosol. PA plus LF produce the lethal toxin (LT), and PA plus EF produce the edema toxin (ET). These toxins cause death and tissue swelling, respectively [8-10]. For more detailed information about the action mechanisms see [6-9, 11-30] and references therein. Due to the power of anthrax spores to endure and their simplicity of production *in vitro*, they are extraordinarily appropriate to be used in aerosol and powdered forms as a natural bioweapon [31-33] (see also [34, 35]). The most appropriate targets for this bioweapon are big cities. To prevent anthrax toxin from functioning, a diversity of approaches has been employed to interfere at different points of its binding, assembly, uptake and mechanism of action. Many compounds have been synthesized and tested for this purpose [36-53]. Recently, a group of 4,6-diamino-2-methylquinoline C-6 amides related to aminoquinuride have been synthesized and tested as inhibitors of the *B. anthracis* lethal factor [53]. Considering the current situation, an approach that could help to understand the microscopic action mechanism of new synthetic compounds seems useful. With this idea, we present here the results of a quantum-chemical analysis of the relationship between electronic structure and the anti-LF activity of the aforementioned molecules.

METHODS, MODELS AND CALCULATIONS

As the formal model (called the Klopman-Peradejordi-Gómez or KPG method) relating electronic structure with biological activity has been presented and discussed in many publications we present here only the final results [54-65]. The logarithm of a biological activity (BA) is related to a set of local atomic reactivity indices (LARIs) by the following linear equation:

$$\log(\mathrm{BA}) = a + \sum_j \left[e_j Q_j + f_j S_j^E + s_j S_j^N \right] + \\ + \sum_j \sum_m \left[h_j(m) F_j(m) + x_j(m) S_j^E(m) \right] + \sum_j \sum_{m'} \left[r_j(m') F_j(m') + t_j(m') S_j^N(m') \right] + \\ + \sum_j \left[g_j \mu_j + k_j \eta_j + o_j \omega_j + z_j \varsigma_j + w_j Q_j^{\max} \right] \quad (1)$$

where a, e_j, f_j, etc., are constants to be determined. Then, for n molecules we have a system of n linear equations 1. As the definition and physical meaning of the LARIs have been discussed before [59, 60], we will only explain in detail those appearing in the results below. This model was originally developed for drug-receptor equilibrium constants but it has been recently (2012) proved to be very successful when applied to other kinds of biological activities [61-80].

ISSN: 0975-8585

The chosen biological activity to be studied here is the inhibition of *Bacillus anthracis* lethal factor (LF) by a series of recently synthesized and tested small molecules [53]. These molecules and their LF inhibitory activities are shown in Fig. 1 and Table 1.

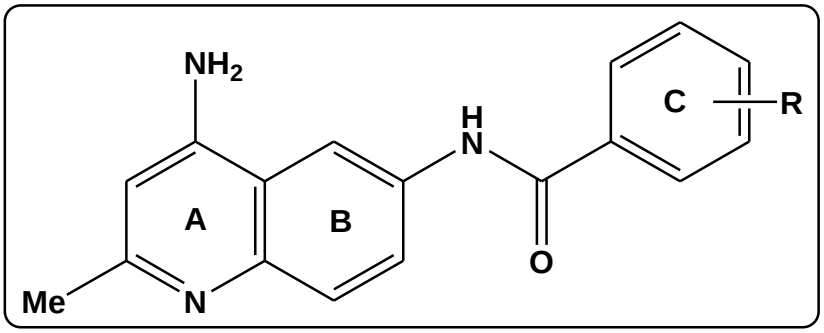

Figure 1: General formula of selected molecules.

Table 1: Molecules and *B. anthracis* Lethal Factor inhibitory activity.

Mol.	log(LF)	R	Mol.	log(LF)	R
1	1.85	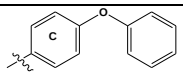	10	1.11	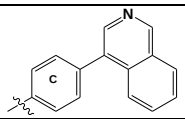
2	1.86	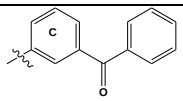	11	1.00	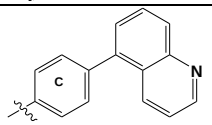
3	1.72	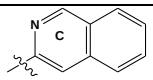	12	1.04	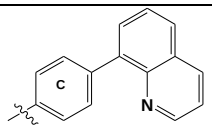
4	1.91	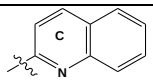	13	0.66	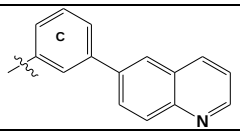
5	1.68	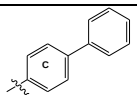	14	0.76	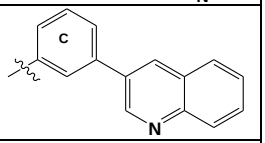
6	1.63	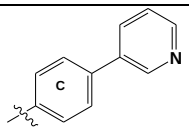	15	1.32	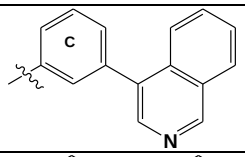
7	0.20	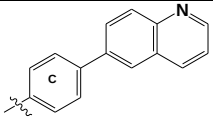	16	1.52	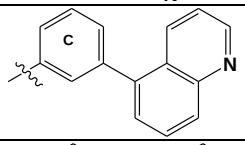
8	1.23	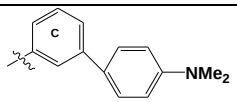	17	1.56	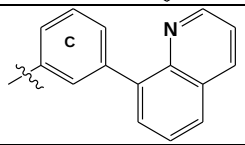
9	0.48	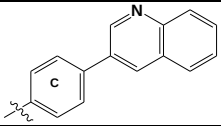			

ISSN: 0975-8585

The calculation of the electronic structure was carried out within DFT at the B3LYP/6-31G(d,p) level of theory after full geometry optimization using the Gaussian suite of programs [81]. The values of the LARIs were calculated with the D-CENT-QSAR software after correction of negative electron populations arising from Mulliken population analysis [82, 83]. We assumed that a set of atoms common to all molecules analyzed (called the common skeleton) encodes the variation of the biological activity throughout the series. Due to the fact that the system of linear equations cannot be directly solved because there are not enough molecules, we employed Linear Multiple Regression Analysis (LMRA) to detect the atoms and properties involved in the variation of the biological activity [84]. The common skeleton numbering is shown in Fig. 2.

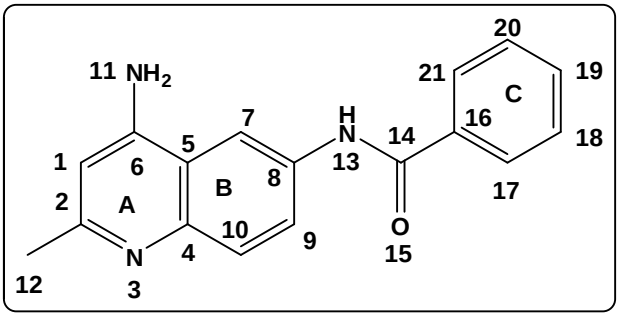

Figure 2: Common skeleton with atom numbering. Atoms 21 in molecule 3 and atom 17 in molecule 4 are nitrogen ones.

RESULTS

The best equation obtained is:

$$\log(IC_{50}) = -4.16 + 1.23\eta_{19} - 0.07S_7^N(LUMO+1)^* - 16.49F_{12}(LUMO)^* \quad (2)$$

with n=17, R=0.93, R^2=0.87, adj-R^2=0.84, F(3,13)=28.07 (*p<0.00001*) and SD=0.21. No outliers were detected and no residuals fall outside the ±2σ limits. Here η_{19} is the local atomic hardness of atom 19, $S_7^N(LUMO)^*$ the nucleophilic superdelocalizability of the lowest vacant MO localized on atom 7 and $F_{12}(LUMO)^*$ the Fukui index (electron population) of the lowest vacant MO localized on atom 12. Tables 2 and 3 show, respectively, the beta coefficients, the results of the t-test for significance of coefficients and the matrix of squared correlation coefficients for the variables appearing in Eq. 2. Table 3 shows that there are no significant internal correlations between independent variables.

Table 2: Beta coefficients and *t*-test for significance of the coefficients in Eq. 2.

	Beta	t(13)	p-level
η_{19}	0.69	6.69	<0.00002
$S_7^N(LUMO+1)^*$	-0.49	-4.77	<0.0004
$F_{12}(LUMO)^*$	-0.35	-3.36	<0.005

Table 3: Squared correlation coefficients for the variables appearing in Eq. 2.

	$S_7^N(LUMO+1)^*$	$F_{12}(LUMO)^*$	η_{19}
$S_7^N(LUMO+1)^*$	1.00		
$F_{12}(LUMO)^*$	0.03	1.00	
η_{19}	0.004	0.02	1.00

ISSN: 0975-8585

DISCUSSION

Linear Multiple Regression Results

The associated statistical parameters of Eq. 2 show that this equation is statistically significant and that the variation of a set of three local atomic reactivity indices belonging to the common skeleton (Fig. 2) explains about 84% of the variation of the anti-LF activity. Fig. 3 shows the plot of predicted *vs*. observed log(IC_{50}) values. Let us remember that all LARIs making a contribution to the anti-LF activity, but having almost the same numerical value, do not appear in the equation.

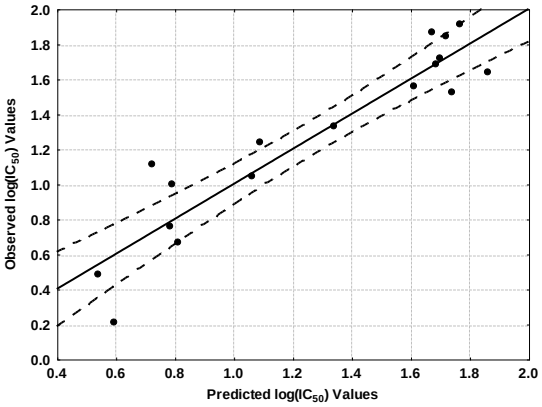

Figure 3: Observed *vs.* predicted values (Eq. 2) of log (IC_{50}). Dashed lines denote the 95% confidence interval.

We can see in Fig. 3 that two cases lie relatively far from the 95% confidence interval. This could be interpreted by suggesting that in these two cases one or more interactions could occur via atoms that do not belong to the common skeleton. More experimental data are needed to test this hypothesis. The beta values (Table 2) show that the importance of the variables is $\eta_{19} > S_7^N(LUMO+1)^* > F_{12}(LUMO)^*$. A variable-by-variable (VbV) analysis indicates that good inhibitory activity is associated with a low value for η_{19} and $F_{12}(LUMO)^*$. As is well known, ab initio, DFT and some semiempirical methods produce one or more vacant MOs with negative associated eigenvalues. For this reason $S_7^N(LUMO+1)^*$ could have a negative or positive value. In the case of Eq. 2, if positive, the value of $S_7^N(LUMO+1)^*$ should be high and, if negative, $\left|S_7^N(LUMO+1)^*\right|$ should be low. A low value for η_{19} indicates that atom C-19 must be a good electrophile. This strongly suggests that C-19 interacts with an electron-rich center. If we consider the position of C-19 (see Fig. 2) we may propose that this interaction involves π-π stacking. A high value of $F_{12}(LUMO)^*$ is associated with good anti-LF activity. C-12 is a methyl substituent belonging to ring A (Fig. 1). $(LUMO)_{12}^*$ is of σ nature. We suggest that $(LUMO)_{12}^*$ interacts with a vacant σ MO (occupied and vacant σ MOs are found in methylene chains for example). In the case of C-7, its first two lowest vacant local MOs are of π nature. The numerical values of $S_7^N(LUMO+1)^*$ are negative in all molecules. A low value for $\left|S_7^N(LUMO+1)^*\right|$ is obtained by lowering the value of the Fukui index (i.e., by diminishing the electron population), or by lowering (i.e., making more negative) the eigenvalue, or by both procedures. In the case of a positive value for $S_7^N(LUMO+1)^*$ this must be high for good anti-LF activity. This can be achieved by lowering the eigenvalue, by raising the Fukui index or both. Considering that in most of the set of molecules we have analogous local atomic reactivity indices with positive and negative values, logics indicates that they must behave similarly. In our case the only common element is the lowering of the MO eigenvalue and the increase of its reactivity. Therefore, more potent anti-LF activity is associated with a more reactive $(LUMO+1)_7^*$ (and $(LUMO)_7^*$). We propose that C-7 participates in a π-π stacking interaction with an electron-rich center. All these ideas are encompassed in the partial two dimensional (2D) anti-LF pharmacophore shown in Fig. 4.

ISSN: 0975-8585

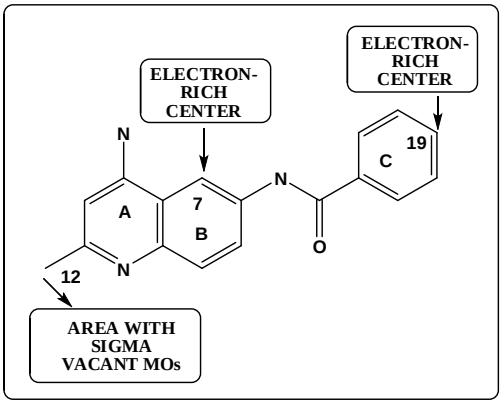

Figure 4: Partial 2D anti-LF pharmacophore built from Eq. 2.

Molecular electrostatic potential (MEP) structure

From the moment that we accept that a common skeleton encodes most, if not all, the biological activity we are implicitly assuming that this skeleton occupies approximately the same position at the site of action. Therefore, if in a statistically significant equation p atoms appear (in the case of Eq. 2 we have three atoms), it is expected that we can build a sort of 3D grid (i.e., a partial pharmacophore) showing these relative positions. In all our papers we have presented only partial 2D pharmacophores because it has not been proved that the fully optimized structure is the one responsible for the biological activity. Moreover, in the case of highly conformationally flexible molecular systems, there are several conformers that can be reached from the fully optimized structure (up to 7 kcal/mol away, for example). Also, it is not possible to demonstrate that a given statistically significant equation contains all the atoms involved in the biological activity. As an example, we show in figures 5 and 6, the MEP maps of molecules 7 and 4 respectively (7 is the most active and 4 the least active of the series, see Table 1) [85].

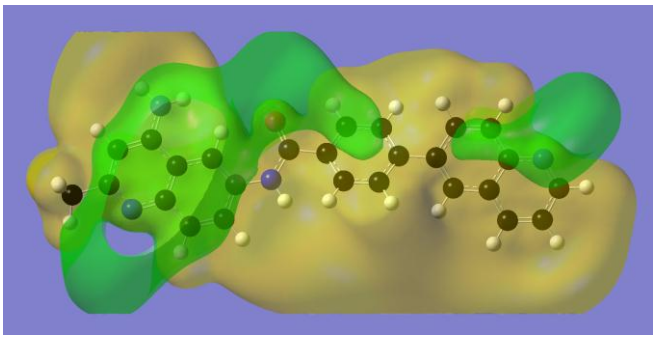

Figure 5: MEP map of molecule 7. The green isovalue surface corresponds to negative MEP values (-0.01) and the yellow isovalue surface to positive MEP values (0.01).

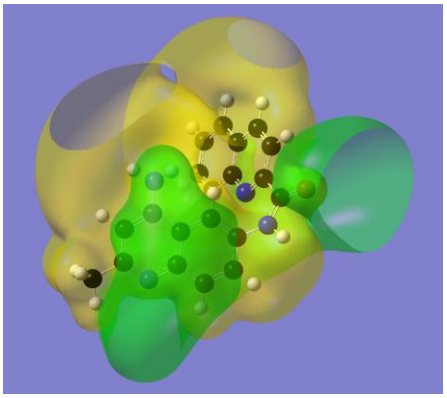

Figure 6: MEP map of molecule 4. The green isovalue surface corresponds to negative MEP values (-0.01) and the yellow isovalue surface to positive MEP values (0.01).

ISSN: 0975-8585

We can see in Fig. 5 that the fully optimized structure of 7 is an extended one while in the case of 4 (Fig. 6) the fully optimized structure is a folded one. Figure 7 shows that if we superimpose rings A-B of both structures atom C-19 does not occupy the same relative position [86].

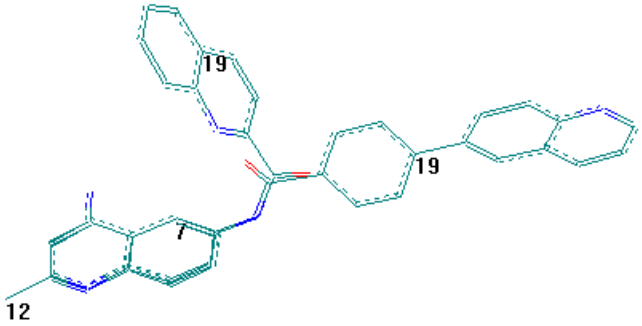

Figure 7: Superimposition of molecules 7 and 4. Numbered atoms are the ones appearing in Eq. 2.

Conformers

Figures 8 and 9 show the superimposition of the ten lowest energy conformers of molecules 7 and 4, respectively. They were calculated with MarvinView (Dreiding force field) [87].

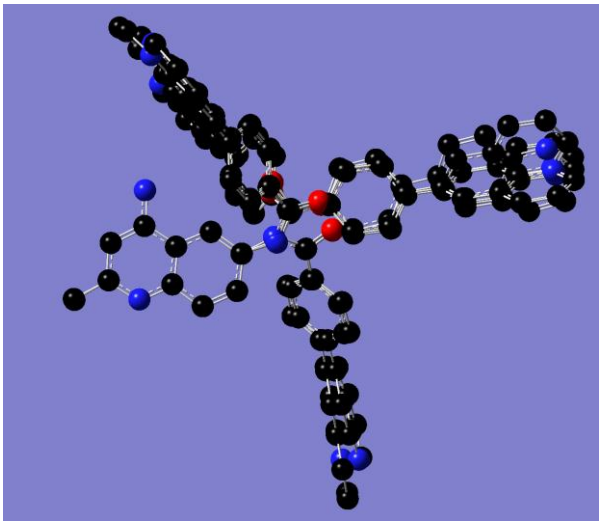

Figure 8: Superimposition of the ten lowest energy conformers of molecule 7.

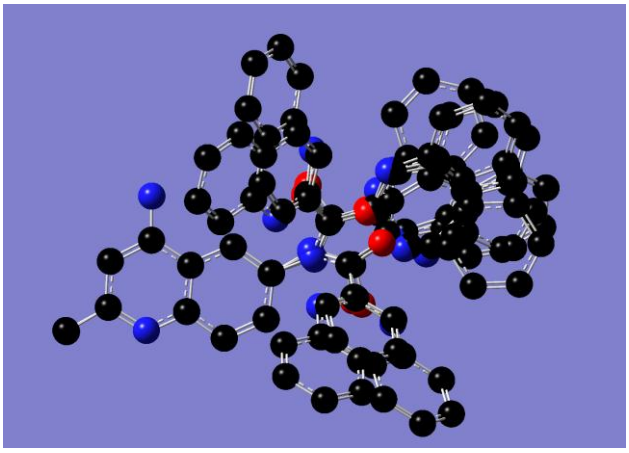

Figure 9: Superimposition of the ten lowest energy conformers of molecule 4.

We can see that both molecules present extended and folded conformers. In a liquid milieu, such as the experimental setting to measure the anti-LF activity, when interacting with LF or within a living structure, it seems likely that the most extended conformers are more stable. Eq. 12 suggests that there is a π-π stacking interaction via C-7 requiring a free area below or above ring B (most of these interactions occur between parallel aromatic rings), allowing us to discard some folded conformers. With the presently available information it is difficult at this point to suggest which might be the active conformer.

On building "hybrids"

In their work, Peet et al. note that molecules 7 and 18 (see below) present high anti-LF activity [53]. By superimposing the corresponding planar (ChemDraw?) structures they propose a "hybrid" that "*we envisioned might incorporate the important recognition elements from both 18 and 7*". Fig. 10 shows both molecules and the proposed hybrid.

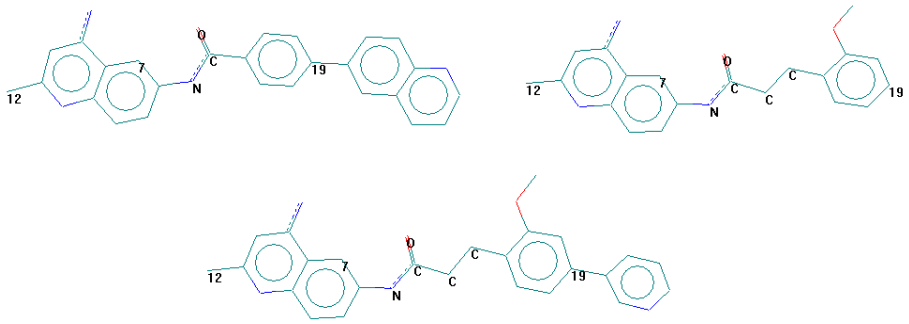

Figure 10: Fully optimized B3LYP/6-31G(d,p) structures of molecules 7 (upper left, LF=1.6 μM), 18 (upper right, LF=3.9 μM) and 19 (below, LF=55 μM).

Concerning the structure-activity analysis that the Peet et al. carried out to detect "*recognition elements*", we have stated that "*papers reporting the synthesis and experimental biological activity of a series of compounds are also bedeviled with loose statements about the relationships between structure and activity. 'If we exchange substituent X for substituent Y, activity Z decreases' is their general form. Such statements are merely the verbal translation of experimental results usually presented in a Table and explain nothing. The situation becomes worse when these statements are accompanied by others of the kind 'activity Z decreases because substituent Y has a stronger inductive effect than substituent X' (from Mid-20th Century Organic Chemistry). The lack of an understanding that, in general, biological activity is encoded in the entire molecular structure and that the mere substitution of a hydrogen atom by a methyl group can affect the whole electronic structure of the molecule (by adding several sigma molecular orbitals and also modifying the eigenvalue spectrum) and not only the area neighboring the point of substitution, leads to these simplistic analyses. For a clear understanding of molecular phenomena the use of quantum chemistry is mandatory*" [78]. Then it is not surprising that the proposed hybrid had a considerably lower anti-LF activity than its putative parents [53]. Let us see if our model performs better. In Fig. 2 we can see that the chosen molecules employed to obtain Eq. 2 have the structure (NH)(CO)-Ring C. Eq. 2 identifies atoms C-7, C-12 and C-19 as three points participating in the anti-LF action. On the other hand, molecules 18 and 19 have an (NH)(CO)(CH_2)(CH_2)-ring C structure. This difference prevents us from using Eq. 2 to predict the anti-LF activities of 18 and 19. Now, note that atoms C-7 and C-12 are common to all three molecules (Fig. 10), but atom C-19 of the common skeleton is not at exactly the same place as the possibly equivalent C-19 in molecules 18 and 19 due to the (CH_2)(CH_2) spacer. Now we have reasoned as follows. We hypothesized that, despite the presence of the enlarged linker joining rings A-B and C, in molecules 18 and 19 C-19 interacts with the same site as C-19 of the set we used to obtain Eq. 2 (see Fig. 10). *If this hypothesis is correct* a LMRA carried out with the original set of Table 1 enlarged with the addition of molecules 18 and 19 should provide a statistically significant equation. After the corresponding LMRA procedure the following equation was obtained:

$$\log(IC_{50}) = 5.24 - 0.67F_4(HOMO-2)^* - 2.54\omega_{10} - 0.02S_{17}^N(LUMO+1)^* - \\ -0.88F_{18}(LUMO+1)^* \quad (3)$$

ISSN: 0975-8585

with N=19, R= 0.95, R^2= 0.90, adjusted R^2= 0.88, F(4,14)=32.901 (p<0.000001) and a standard error of estimate of 0.19. No outliers were detected and no residuals fall outside the ±2σ limits. Here, $F_4(HOMO-2)^*$ is the Fukui index of the third highest occupied MO localized on atom 4, ω_{10} is the local atomic electrophilicity of atom 10, $S_{17}^N(LUMO+1)^*$ is the orbital nucleophilic superdelocalizability of the second lowest vacant MO localized on atom 17 and $F_{18}(LUMO+1)^*$ is the Fukui index of the second lowest vacant MO localized on atom 18. Tables 4 and 5 show, respectively, the beta coefficients, the results of the t-test for significance of coefficients and the matrix of squared correlation coefficients for the variables appearing in Eq. 3. Table 5 shows that there are no significant internal correlations between independent variables. The associated statistical parameters of Eq. 3 show that this equation is statistically significant and that the variation of a group of three local atomic reactivity indices belonging to the common skeleton explains about 88% of the variation of the anti-LF activity. Fig. 11 displays the plot of predicted *vs*. observed log(IC_{50}) values.

Table 4: Beta coefficients and *t*-test for significance of the coefficients in Eq. 3.

	Beta	B	t(14)	p-level
$F_4(HOMO-2)^*$	-0.74	-0.67	-7.96	<0.000001
ω_{10}	-0.68	-2.54	-6.46	<0.00002
$S_{17}^N(LUMO+1)^*$	-0.54	-0.02	-5.84	<0.00004
$F_{18}(LUMO+1)^*$	-0.29	-0.88	-3.28	<0.005

Table 5: Squared correlation coefficients for the variables appearing in Eq. 3.

	$F_4(HOMO-2)^*$	ω_{10}	$S_{17}^N(LUMO+1)^*$
ω_{10}	0.19	1.00	
$S_{17}^N(LUMO+1)^*$	0.07	0.20	1.00
$F_{18}(LUMO+1)^*$	0.002	0.12	0.02

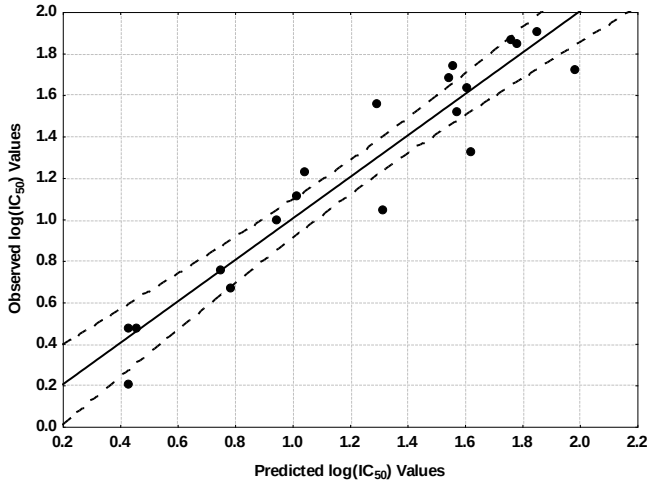

Figure 11: Observed *vs.* predicted values (Eq. 3) of log (IC_{50}). Dashed lines denote the 95% confidence interval.

The beta values (Table 4) show that the importance of the variables is $F_4(HOMO-2)^* > \omega_{10} > S_{17}^N(LUMO+1)^* > F_{18}(LUMO+1)^*$. A variable-by-variable (VbV) analysis shows that good anti-LF

ISSN: 0975-8585

activity is associated with high values for $F_4(HOMO-2)^*$, ω_{10} and $F_{18}(LUMO+1)^*$. In this enlarged set all molecules but 18 have negative values for $S_{17}^N(LUMO+1)^*$. When negative, the values of $\left|S_{17}^N(LUMO+1)^*\right|$ should be low for good anti-LF activity and, when positive, $S_{17}^N(LUMO+1)^*$ values should be high. A high value for ω_{10} indicates that C-10 (Fig. 2) should behave as a good electrophile, indicating that this atom interacts with an electron-rich moiety. A high value for $F_{18}(LUMO+1)^*$, a local MO of π nature, suggests that C-18 also interacts with an electron-rich center. $(HOMO-2)_4^*$ is of π nature in all molecules. Then a high value for $F_4(HOMO-2)^*$ is indicative of an interaction of C-4, through its first three highest occupied MOs, with an electron-deficient center. Using the same considerations applied to the analysis of $S_7^N(LUMO+1)^*$ in Eq. 2, potent anti-LF activity is associated with a more reactive $(LUMO+1)_{17}^*$ (and $(LUMO)_{17}^*$). Then, atom 17 interacts, through its two lowest vacant MOs, with an electron-rich center. These ideas are condensed in the 2D anti-LF pharmacophore shown in Fig. 12.

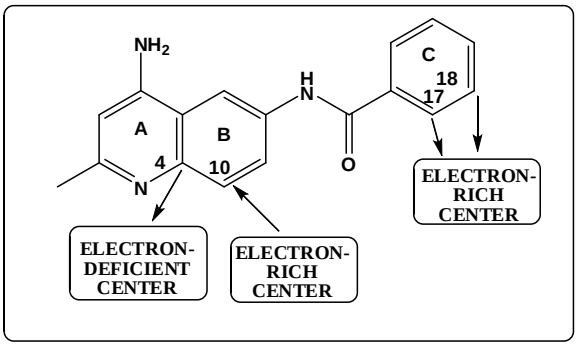

Figure 12: Partial 2D anti-LF pharmacophore built from Eq. 3.

If we merge both pharmacophores (Figs. 4 and 12), we obtain the one shown in Fig. 13.

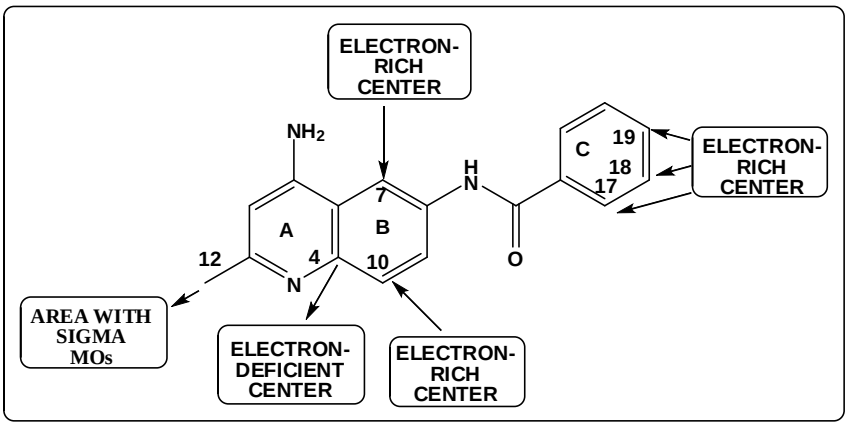

Figure 13: Partial 2D anti-LF pharmacophore built from Eqs. 2 and 3.

We can see that, as expected, the final partial 2D pharmacophore does not contain contradictory elements. The results strongly suggest that atoms 19 as shown in Fig. 10 could be a common element in an enlarged common skeleton. We think that these results show the superiority of the model employed here over the statistics-only-methods [88]. Also, given present-day computational capabilities and the availability of quantum chemistry software, there is no reason to avoid the daily use of this tool.

ACKNOWLEDGEMENTS

Prof. Dr. Bruce K. Cassels (Faculty of Sciences, University of Chile) is thanked for helpful comments.

REFERENCES

[1] Stark JF. *The making of modern anthrax, 1875-1920 : uniting local, national and global histories of disease,* Pickering & Chatto, London, 2013.
[2] Viljoen, PR, South Africa. Department of Agriculture., *Anthrax : its nature and control,* Govt. Printing and Stationery Office, Pretoria, 1927.
[3] Guillemin, J, *Anthrax : the investigation of a deadly outbreak,* University of California Press, Berkeley ; London, 1999.
[4] Jones, SD, *Death in a small package : a short history of anthrax,* Johns Hopkins University Press, Baltimore, 2010.
[5] Leppla, SH, "Chapter 281 - Anthrax Lethal Factor," in *Handbook of Proteolytic Enzymes*, N. D. R. Salvesen Ed., pp. 1257-1261, Academic Press, 2013.
[6] Schiffmiller, A. Biophys. J., 2013, 104, 631a.
[7] Kintzer, AF, Thoren, KL, Sterling, HJ, Feld, GK, Tang, II, Krantz, BA. Biophys. J., 2010, 98, 452a-453a.
[8] Liu, S, Moayeri, M, Leppla, SH. Trends Microbiol., 2014, 22, 317-325.
[9] Guichard, A, Nizet, V, Bier, E. Microb. Infect., 2012, 14, 97-118.
[10] Dumetz, F, Jouvion, G, Khun, H, Glomski, IJ, Corre, J-P, Rougeaux, C, Tang, W-J, Mock, M, Huerre, M, Goossens, PL. Amer. J. Pathol., 2011, 178, 2523-2535.
[11] Dennis, MK, Mogridge, J. Biochem., 2014, 53, 2166-2171.
[12] Das, D. Biophys. J., 2014, 106, 50a.
[13] Thomas, J, Metcalf, J, Christman, JW, Cook, J, Levitan, I. Biophys. J., 2013, 104, 132a.
[14] Naik, S, Brock, S, Akkaladevi, N, Tally, J, McGinn-Straub, W, Zhang, N, Gao, P, Gogol, EP, Pentelute, BL, Collier, RJ, Fisher, MT. Biochem., 2013, 52, 6335-6347.
[15] Mukherjee, S, Lee, KI, Zhang, Y, Fisher, M, Im, W. Biophys. J., 2013, 104, 63a.
[16] Jang, J, Cho, M, Lee, H-R, Cha, K, Chun, J-H, Hong, K-J, Park, J, Rhie, G-e. Biochem. Biophys. Acta Gen. Subj., 2013, 1830, 2804-2812.
[17] Abrami, L, Brandi, L, Moayeri, M, Brown, Michael J, Krantz, Bryan A, Leppla, Stephen H, van der Goot, FG. Cell Rep., 2013, 5, 986-996.
[18] Rameshwar, P, Wong, EW, Connell, ND. Cytokine, 2012, 57, 143-149.
[19] Garlick, KM, Batty, S, Mogridge, J. Biochem., 2012, 51, 1249-1256.
[20] Feld, GK, Kintzer, AF, Tang, II, Thoren, KL, Krantz, BA. J. Mol. Biol., 2012, 415, 159-174.
[21] Ahn, HC, Kim, NY, Hur, GH, Yang, JM, Shin, S. Toxicology, 2012, 297, 10-16.
[22] Maddugoda, Madhavi P, Stefani, C, Gonzalez-Rodriguez, D, Saarikangas, J, Torrino, S, Janel, S, Munro, P, Doye, A, Prodon, F, Aurrand-Lions, M, Goossens, Pierre L, Lafont, F, Bassereau, P, Lappalainen, P, Brochard, F, Lemichez, E. Cell Host. Microb., 2011, 10, 464-474.
[23] Ali, Syed R, Timmer, Anjuli M, Bilgrami, S, Park, Eek J, Eckmann, L, Nizet, V, Karin, M. Immunity, 2011, 35, 34-44.
[24] Raymond, B, Ravaux, L, Mémet, S, Wu, Y, Sturny-Leclère, A, Leduc, D, Denoyelle, C, Goossens, PL, Payá, M, Raymondjean, M, Touqui, L. Biochem. Pharmacol., 2010, 79, 1149-1155.
[25] Liu, S, Miller-Randolph, S, Crown, D, Moayeri, M, Sastalla, I, Okugawa, S, Leppla, SH. Cell Host. Microb., 2010, 8, 455-462.
[26] Gu, J, Faundez, V, Werner, E. Experimental Cell Research, 2010, 316, 1946-1957.
[27] Tournier, J-N, Rossi Paccani, S, Quesnel-Hellmann, A, Baldari, CT. Mol. Aspects Med., 2009, 30, 456-466.
[28] Tan, YK, Kusuma, CM, St. John, LJ, Vu, HA, Alibek, K, Wu, A. Biochem. Biophys. Res. Comm., 2009, 379, 293-297.
[29] Moayeri, M, Leppla, SH. Mol. Aspects Med., 2009, 30, 439-455.
[30] Kintzer, AF, Thoren, KL, Sterling, HJ, Dong, KC, Feld, GK, Tang, II, Zhang, TT, Williams, ER, Berger, JM, Krantz, BA. J. Mol. Biol., 2009, 392, 614-629.
[31] Johnstone, RW, *Bioterror : anthrax, influenza, and the future of public health security,* Praeger Security International, Westport, Conn. ; London, 2008.
[32] Lutwick, LI, Lutwick, SM, *Beyond anthrax : the weaponization of infectious diseases,* Springer, New York, 2009.
[33] Watkins, C, *Biological warfare,* Greenhaven Press, Detroit, 2010.
[34] Zhang, X, Kuča, K, Dohnal, V, Dohnalová, L, Wu, Q, Wu, C. J. App. Biomed., 2014, 12, 63-77.
[35] Zapanta, PE, Ghorab, S. Otolaryngology -- Head and Neck Surgery, 2014,

[36] Johnson, SL, Jung, D, Forino, M, Chen, Y, Satterthwait, A, Rozanov, DV, Strongin, AY, Pellecchia, M. J. Med. Chem., 2005, 49, 27-30.
[37] Shultz, CS, Dreher, SD, Ikemoto, N, Williams, JM, Grabowski, EJJ, Krska, SW, Sun, Y, Dormer, PG, DiMichele, L. Org. Lett., 2005, 7, 3405-3408.
[38] Gujraty, KV, Joshi, A, Saraph, A, Poon, V, Mogridge, J, Kane, RS. Biomacromol., 2006, 7, 2082-2085.
[39] Jiao, G-S, Cregar, L, Goldman, ME, Millis, SZ, Tang, C. Bioorg. Med. Chem. Lett., 2006, 16, 1527-1531.
[40] Jiao, G-S, Simo, O, Nagata, M, O'Malley, S, Hemscheidt, T, Cregar, L, Millis, SZ, Goldman, ME, Tang, C. Bioorg. Med. Chem. Lett., 2006, 16, 5183-5189.
[41] Joshi, A, Saraph, A, Poon, V, Mogridge, J, Kane, RS. Bioconj. Chem., 2006, 17, 1265-1269.
[42] Schepetkin, IA, Khlebnikov, AI, Kirpotina, LN, Quinn, MT. J. Med. Chem., 2006, 49, 5232-5244.
[43] Xiong, Y, Wiltsie, J, Woods, A, Guo, J, Pivnichny, JV, Tang, W, Bansal, A, Cummings, RT, Cunningham, BR, Friedlander, AM, Douglas, CM, Salowe, SP, Zaller, DM, Scolnick, EM, Schmatz, DM, Bartizal, K, Hermes, JD, MacCoss, M, Chapman, KT. Bioorg. Med. Chem. Lett., 2006, 16, 964-968.
[44] Gaddis, BD, Avramova, LV, Chmielewski, J. Bioorg. Med. Chem. Lett., 2007, 17, 4575-4578.
[45] Hanna, ML, Tarasow, TM, Perkins, J. Bioinorg. Chem., 2007, 35, 50-58.
[46] Nguyen, TL, Panchal, RG, Topol, IA, Lane, D, Kenny, T, Burnett, JC, Hermone, AR, McGrath, C, Burt, SK, Gussio, R, Bavari, S. J. Mol. Struct. Theochem, 2007, 821, 139-144.
[47] Gaddis, BD, Rubert Pérez, CM, Chmielewski, J. Bioorg. Med. Chem. Lett., 2008, 18, 2467-2470.
[48] Chiu, T-L, Solberg, J, Patil, S, Geders, TW, Zhang, X, Rangarajan, S, Francis, R, Finzel, BC, Walters, MA, Hook, DJ, Amin, EA. J. Chem. Info. Mod., 2009, 49, 2726-2734.
[49] Johnson, SL, Chen, L-H, Barile, E, Emdadi, A, Sabet, M, Yuan, H, Wei, J, Guiney, D, Pellecchia, M. Bioorg. Med. Chem., 2009, 17, 3352-3368.
[50] Roy, J, Kumar, UC, Machiraju, PK, Muttineni, RK, Kumar B.V.S, S, Gundla, R, Dayam, R, Sarma, JARP. J. Mol. Graph. Mod., 2010, 29, 256-265.
[51] Joshi, A, Kate, S, Poon, V, Mondal, D, Boggara, MB, Saraph, A, Martin, JT, McAlpine, R, Day, R, Garcia, AE, Mogridge, J, Kane, RS. Biomacromol., 2011, 12, 791-796.
[52] Jung, ME, Chamberlain, BT, Ho, C-LC, Gillespie, EJ, Bradley, KA. ACS Med. Chem. Lett., 2014, 5, 363-367.
[53] Williams, JD, Khan, AR, Cardinale, SC, Butler, MM, Bowlin, TL, Peet, NP. Bioorg. Med. Chem., 2014, 22, 419-434.
[54] Gómez Jeria, JS. Boll. Chim. Farmac., 1982, 121, 619-625.
[55] Gómez-Jeria, JS. Int. J. Quant. Chem., 1983, 23, 1969-1972.
[56] Gómez-Jeria, JS, "Modeling the Drug-Receptor Interaction in Quantum Pharmacology," in *Molecules in Physics, Chemistry, and Biology*, J. Maruani Ed., vol. 4, pp. 215-231, Springer Netherlands, 1989.
[57] Gómez-Jeria, JS, Ojeda-Vergara, M, Donoso-Espinoza, C. Mol. Engn., 1995, 5, 391-401.
[58] Gómez-Jeria, JS, Ojeda-Vergara, M. J. Chil. Chem. Soc., 2003, 48, 119-124.
[59] Gómez-Jeria, JS, *Elements of Molecular Electronic Pharmacology (in Spanish),* Ediciones Sokar, Santiago de Chile, 2013.
[60] Gómez-Jeria, JS. Canad. Chem. Trans., 2013, 1, 25-55.
[61] Gómez-Jeria, JS. Res. J. Pharmac. Biol. Chem. Sci., 2014, 5, 2124-2142.
[62] Gómez-Jeria, JS. J. Comput. Methods Drug Des., 2014, 4, 32-44.
[63] Gómez-Jeria, JS. Res. J. Pharmac. Biol. Chem. Sci., 2014, 5, 424-436.
[64] Gómez-Jeria, JS, Molina-Hidalgo, J. J. Comput. Methods Drug Des., 2014, 4, 1-9.
[65] Solís-Gutiérrez, R, Gómez-Jeria, JS. Res. J. Pharmac. Biol. Chem. Sci., 2014, 5, 1401-1416.
[66] Barahona-Urbina, C, Nuñez-Gonzalez, S, Gómez-Jeria, JS. J. Chil. Chem. Soc., 2012, 57, 1497-1503.
[67] Bruna-Larenas, T, Gómez-Jeria, JS. Int. J. Med. Chem., 2012, 2012 Article ID 682495, 1-16.
[68] Alarcón, DA, Gatica-Díaz, F, Gómez-Jeria, JS. J. Chil. Chem. Soc., 2013, 58, 1651-1659.
[69] Gómez-Jeria, JS, Flores-Catalán, M. Canad. Chem. Trans., 2013, 1, 215-237.
[70] Paz de la Vega, A, Alarcón, DA, Gómez-Jeria, JS. J. Chil. Chem. Soc., 2013, 58, 1842-1851.
[71] Reyes-Díaz, I, Gómez-Jeria, JS. J. Comput. Methods Drug Des., 2013, 3, 11-21.
[72] Gómez-Jeria, JS. Int. Res. J. Pure App. Chem., 2014, 4, 270-291.
[73] Gómez-Jeria, JS. Der Pharm. Lett., 2014, 6., 95-104.
[74] Gómez-Jeria, JS. Brit. Microbiol. Res. J., 2014, 4, 968-987.
[75] Gómez-Jeria, JS. SOP Trans. Phys. Chem., 2014, 1, 10-28.
[76] Gómez-Jeria, JS. Der Pharma Chem., 2014, 6, 64-77.
[77] Muñoz-Gacitúa, D, Gómez-Jeria, JS. J. Comput. Methods Drug Des., 2014, 4, 33-47.
[78] Muñoz-Gacitúa, D, Gómez-Jeria, JS. J. Comput. Methods Drug Des., 2014, 4, 48-63.

[79] Pino-Ramírez, DI, Gómez-Jeria, JS. Amer. Chem. Sci. J., 2014, 4, 554-575.
[80] Salgado-Valdés, F, Gómez-Jeria, JS. J. Quant. Chem., 2014, 2014 Article ID 431432, 1-15.
[81] Frisch, MJ, Trucks, GW, Schlegel, HB, Scuseria, GE, Robb, MA, Cheeseman, JR, Montgomery, J, J.A., Vreven, T, Kudin, KN, Burant, JC, Millam, JM, Iyengar, SS, Tomasi, J, Barone, V, Mennucci, B, Cossi, M, Scalmani, G, Rega, N. Gaussian98 Rev. A.11.3, Gaussian, Pittsburgh, PA, USA, 2002.
[82] Gómez-Jeria, JS. D-Cent-QSAR: A program to generate Local Atomic Reactivity Indices from Gaussian log files. 1.0, Santiago, Chile, 2014.
[83] Gómez-Jeria, JS. J. Chil. Chem. Soc., 2009, 54, 482-485.
[84] Statsoft. Statistica 8.0, 2300 East 14 th St. Tulsa, OK 74104, USA, 1984-2007.
[85] Dennington, RD, Keith, TA, Millam, JM. GaussViev 5.0.8, GaussViev 5.0.8, 340 Quinnipiac St., Bldg. 40, Wallingford, CT 06492, USA, 2000-2008.
[86] Hypercube. Hyperchem 7.01, 419 Phillip St., Waterloo, Ontario, Canada, 2002.
[87] Chemaxon. MarvinView, www.chemaxon.com, USA, 2014.
[88] Martin, YC, *Quantitative drug design: a critical introduction,* M. Dekker, New York, 1978.